Structural and gas adsorption study of a two-dimensional copper–tetrazole based metal–organic framework

Pradip Pachfule and Rahul Banerjee*

Physical/Materials Chemistry Division, National Chemical Laboratory, Dr Homi Bhabha Road, Pune 411 008, India

A new two-dimensional (2D) metal–organic framework, $Cu_1(4\text{-}TBA)_1(DMBP)_1\cdot DMF$ (Cu-TBA-3), has been synthesized under solvothermal condition from transition metal cation Cu(II), predesigned ligand 4-(1H-tetrazole-5-yl)benzoic acid (4-TBA) and coligand 4,4′-dimethyl-2,2′-bipyridine (DMBP). The structure has been determined by single crystal X-ray crystallography which shows layered 2D structure with square shaped one-dimensional channels. Cu-TBA-3 shows 0.69 wt% H_2 (at 77 K, 1 atm) and 1.65 mmol/g CO_2 (at 298 K, 1 atm) uptake.

Keywords: CO_2 capture, hydrogen storage, metal–organic frameworks, microporous materials.

METAL–ORGANIC frameworks (MOFs)[1] represent a new class of network solids that have great potential in specific applications such as separation[2], storage[3], heterogeneous catalysis[4] and controlled drug delivery[5]. Extensive research has been performed on MOFs as these materials are excellent for storing hydrogen[6] and carbon dioxide[7]. It is noteworthy that, active research for storing hydrogen is being carried out on functionalized and non-functionalized carbon nanotubes[8], zeolites[9], activated carbon[10] and metal hydrides[11]. Although these materials have been extensively studied and potentially applied in several ways, their use is limited as they are expensive, show strong interaction with adsorbents and regeneration of adsorbents is not easy. MOFs on the other hand have shown promise over these materials owing to their fascinating structures, exceptionally high surface areas, uniform yet tunable pore sizes and well-defined adsorbate–MOF interaction sites[12]. A common design strategy for MOF materials uses rigid and extended organic ligands such as carboxylates and polypyridines as organic backbone. However, other ligands especially nitrogen-containing heterocyclic compounds (e.g. pyrazole, imidazoles, triazoles and tetrazoles), have been exploited in the construction of complex metal organic architectures[13]. As these links are small in size, by adjusting the shape, flexibility, length, and symmetry, a remarkable range of MOFs containing various architectures and functions can be prepared. Particularly, ligands having tetrazole/triazole/imidazole and carboxylic groups available for co-ordination are important because: (i) they possess multiple functional groups with different coordination modes. The carboxylate and tetrazole/triazole/imidazole group can adopt versatile coordination conformations, from monodentate to tetradentate. Combination of both these functionalities can create a number of new MOFs with uncommon topologies. (ii) Elongated structure of the ligand with carboxylate and tetrazole/triazole/imidazole functionality can create large pores for gas adsorption.

Herein, we report structural analysis and gas adsorption studies of a porous MOF synthesized from multidentate ligand 4-(1H-tetrazole-5-yl)benzoic acid (4-TBA), coligand 4,4′-dimethyl-2,2′-bipyridine (DMBP) and transition metal ion Cu(II) as a metal centre in DMF solvent (Scheme 1). The MOF synthesized can be formulated as [Cu1(4-TBA)1$(DMBP)_1\cdot$DMF] (Cu-TBA-3) (DMF, dimethyl formamide) displays an interesting two-dimensional (2D) architecture containing trapped DMF molecules inside the pores. The structure of Cu-TBA-3 has been determined by single crystal X-ray crystallography and further identified by infrared (IR) spectroscopy, powder X-ray diffraction (PXRD) and thermal gravimetric analysis (TGA). The adsorption properties H_2 and CO_2 at 77 K and 298 K have been analysed.

The ligand 4-TBA was synthesized according to the modified literature procedure[14]. As 4-TBA is sparingly soluble in water at moderate temperature, we used the solvent DMF in which it is readily soluble. Further, its reaction with $Cu(NO_3)_2\cdot 3H_2O$ at room temperature results in the formation of microcrystalline precipitate of Cu-TBA-3. So, we used the solvothermal condition (at 85°C) for synthesis which results in the formation of single crystals suitable for X-ray diffraction. To a stock solution of 1.5 ml 4-TBA (0.20 M) and 0.5 ml DMBP (0.20 M) 0.5 ml, $Cu(NO_3)_2\cdot 3H_2O$ (0.20 M) was added. To this solution was added 0.5 ml of absolute ethanol. The vial was capped and heated to 85°C for 96 h (Scheme 2). The mother liquor was decanted and the products were washed with DMF (15 ml) thrice. The synthesized Cu-TBA-3 is stable and insoluble in common organic solvents. Further thermal stability and phase purity of the synthesized bulk compound was checked by TGA and PXRD.

*For correspondence. (e-mail: r.banerjee@ncl.res.in)

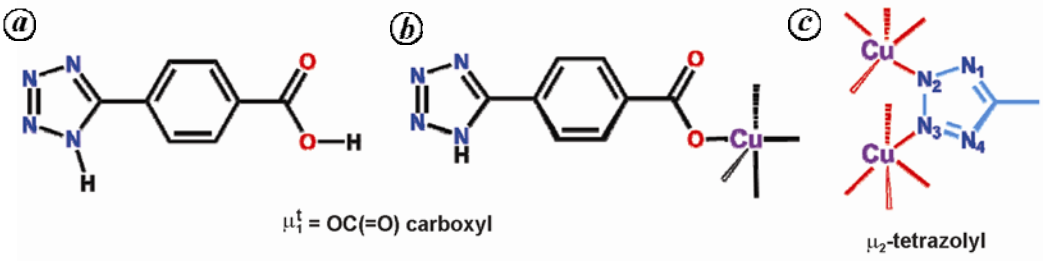

Scheme 1. Schematic drawing and mode of coordination of 4-TBA links observed in Cu-TBA-3. ***a***, Schematic drawing of 4-(1H-tetrazole-5-yl)benzoic acid or 4-tetrazole benzoic acid (4-TBA). ***b***, μ_1^t–CO(=O) coordination mode for carboxylic group. ***c***, μ_2-tetrazolyl coordination mode for tetrazolyl group.

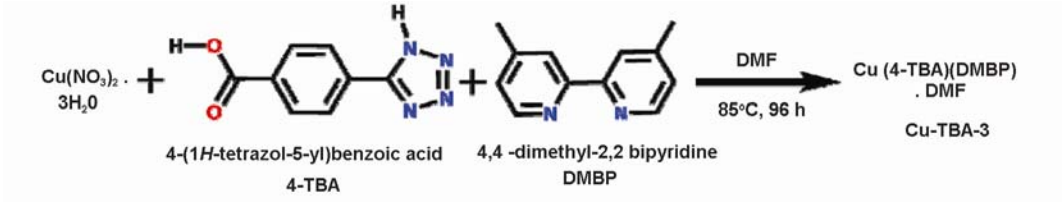

Scheme 2. Scheme of synthesis for Cu-TBA-3 MOF.

The asymmetric unit of Cu-TBA-3 (space group $P2_1/c$) consists of one crystallographically independent pentacoordinated Cu^{2+} ion, one 4-TBA, one DMBP and one lattice DMF molecule (Figure 1 *a* and Scheme 1). Each Cu^{2+} ion is surrounded by one oxygen (Cu–O = 1.920 Å) from μ_1^t-OC(=O) carboxyl group and four nitrogen atoms from one chelating DMBP, two μ_2-tetrazolyl group from 4-TBA ligands through N_2 and N_3 atoms, where Cu–N distances range from 1.971(2) to 2.274(3) Å (Figure 1 *a*). In the structure Cu–N_{DMBP}, distance (1.971(2) Å) is shorter than Cu–$N_{Tetrazole}$ distance (2.274(3) Å), as it originates from the deprotonated tetrazole ring. In the structure of Cu-TBA-3, each secondary binding unit (SBU) connects to the next SBU through the nitrogen atom of the μ_2-tetrazole group and the oxygen from μ_1^t-OC(=O) carboxyl group extends further through the μ_2-tetrazole group of 4-TBA (Figure 1 *c*). As the DMBP possesses two coordinating nitrogen atoms which are joined to the same Cu^{2+} atom, the structure does not extend in the crystallographic *a* axis, as co-coordinating sites are blocked by the DMBP (Figure 1 *b*). Cu-TBA-3, structure extends through the carboxyl and tetrazolyl group of 4-TBA, through *b* and *c* axis, providing 2D architecture with one-dimensional (1D) channels of 3.471 × 8.124 Å dimensions along *a* axis (Figure 1 *d*). The structure contains interesting square 1D channels, with uncoordinated DMF molecules inside the pore. The calculations using PLATON[15] suggest that solvent accessible void in the Cu-TBA-3 is as high as 49.0% after removing the guest DMF molecules.

To examine the architectural and thermal stability of Cu-TBA-3 reported in this article, we prepared them at the gram scale to allow detailed study of the aforementioned properties. TGA performed on the synthesized Cu-TBA-3 revealed that this compound has high thermal stability (see in Supplementary material, for data and interpretations regarding guest mobility and thermal stability of Cu-TBA-3). The TGA trace for Cu-TBA-3 showed a gradual weight-loss step of ~11.2% (15–200°C), corresponding to escape of all DMF in the pores (1 DMF; calcd. ~15.43%) followed by a sharp weight loss (200–450°C) probably owing to the decomposition of the coordinated DMBP molecules before decomposition of the framework as shown in Figure 2 *a*. After 450°C, the framework breaks yielding nearly 25% residues.

To confirm the phase purity of the bulk materials, PXRD experiments were carried out on Cu-TBA-3. The PXRD of experimental and computer-simulated patterns of Cu-TBA-3 is shown in Figure 2 *b*. As shown in figures, all major peaks of the experimental PXRDs patterns of the compound Cu-TBA-3 match well with those of simulated PXRDs, indicating their reasonable crystalline phase purity. The experimental pattern of Cu-TBA-3 has a few diffraction lines that are unindexed and some that are slightly broadened in comparison with those simulated patterns. This is probably because of the loss of DMF molecules from the lattice owing to grinding during preparation of samples, before collecting the PXRD data.

From the crystalline structure of Cu-TBA-3 (Cu-TBA-3: C22.46 H16 N6.34 O2.23 Cu, M_r = 473.96, Monoclinic, P21/*c*, a = 10.594(16) Å; b = 15.10(2) Å; c = 20.05(3); V = 3195(8) Å^3, D_c = 0.985 g cm^{-3}, μ = 0.707 mm^{-1}, 5487 total reflection, 1788 unique (R_{int} = 0.0421), T = 293(2), final R indices ($I > 2\sigma(I)$): R_1 = 0.0964, wR_2 = 0.2216, Goodness-of-fit = 0.876. CCDC 826508), it is confirmed that Cu-TBA-3 have pores of 3.471 × 8.124 Å diameter, so we concentrated on the gas adsorption studies of Cu-TBA-3. Recently researchers investigated that, solvent-free frameworks are more useful for gas adsorption.

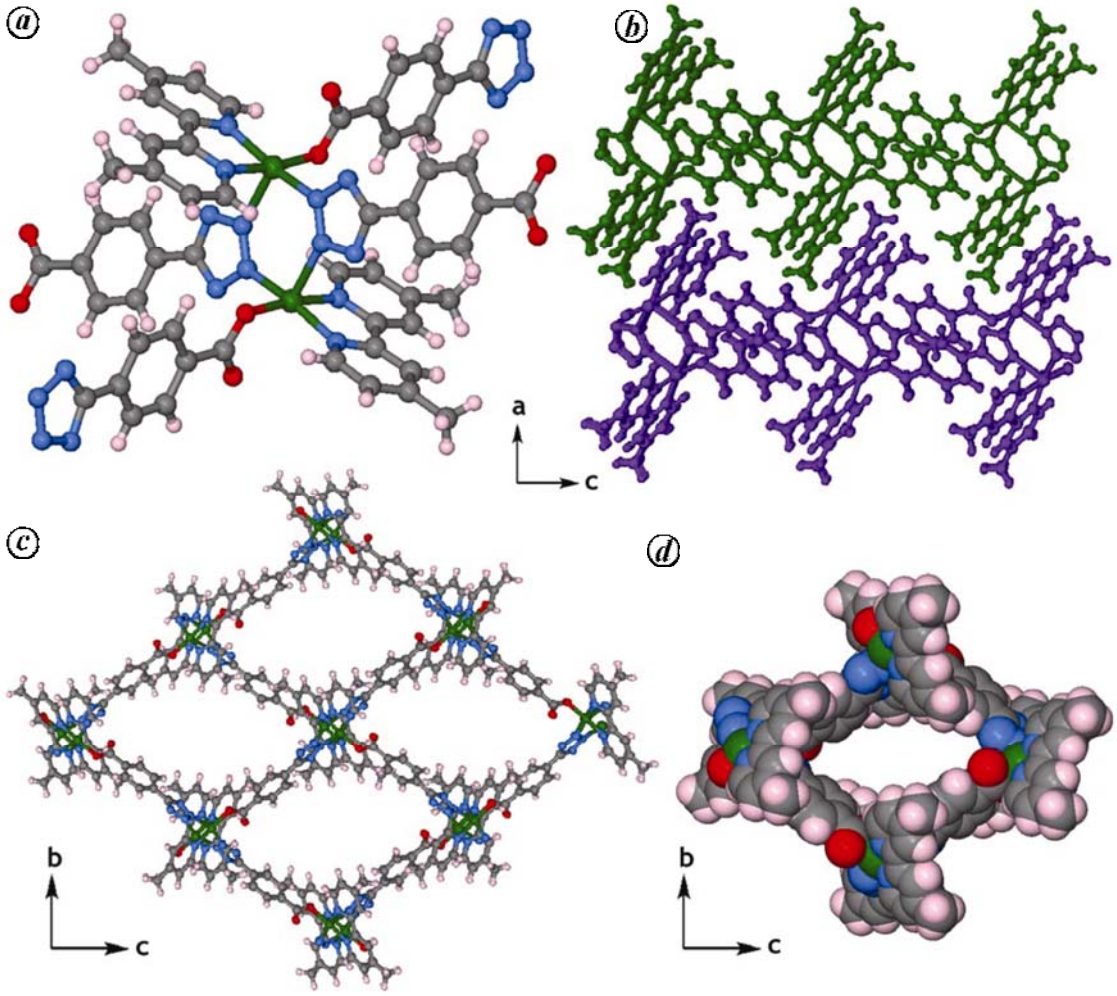

Figure 1. Schematic drawing for crystal structure of $Cu_1(4\text{-TBA})_1(DMBP)_1{\cdot}DMF$ (Cu-TBA-3). ***a***, Tetragonal pyramidal type SBU (1 oxygen and 4 nitrogen atoms) of Cu-TBA-3. ***b***, In the 2D structure of Cu-TBA-3, each layer separates from the other owing to blocking of the co-ordination sites of Cu^{2+} by DMBP molecules. ***c***, 1D square channels of 3.471 × 8.124 Å dimensions extending through *a* axis. ***d***, Packing diagram showing formation of hollow cages formation through *a* axis. Solvent molecules are omitted for clarity. Colour code: Cu (green), N (blue), O (red), C (black), H (pink).

Table 1. Crystal data and structure refinement for Cu-TBA-3

	Cu-TBA-3
Empirical formula	C22.46 H16 N6.34 O2.23Cu
Formula weight	473.96
Crystal system	Monoclinic
Space group	$P2_1/c$
Unit cell dimensions	a = 10.594(16) Å, b = 15.10(2) Å, c = 20.05(3) Å, β = 95.01(2)°
Volume	3195(8)
Z	4
Density (calculated)	0.985
Reflections collected	5487
Independent reflections	1788
Data/restraints/parameters	5487/0/270
Goodness-of-fit on F^2	0.876
Final R indices [$I > 2\sigma(I)$]	R_1 = 0.0964, wR_2 = 0.2216
R indices (all data)	R_1 = 0.2658, wR_2 = 0.3041
Largest diff. peak and hole	0.085 and –0.485 eÅ^{-3}

So, the synthesized sample of Cu-TBA-3 was immersed in dry chloroform at ambient temperature for 72 h, evacuated at ambient temperature for 24 h, then at an elevated temperature 100°C for 36 h under ultrahigh vacuum (10^{-8} mbar) overnight, to create solvent-free framework. Samples thus obtained were optimally evacuated, as evidenced by their well-maintained PXRD patterns and the long plateau (ambient temperature to 350°C) in their TGA traces.

Cu-TBA-3 is non-porous to N_2 because its aperture size is less than the kinetic diameter of N_2 (3.6 Å), however Cu-TBA-3 is porus to H_2 (2.89 Å) and CO_2 (3.3 Å) as it has less kinetic diameter compared to N_2. Further, the low kinetic energy of the N_2 molecules at 77 K results in N_2 molecules that are unable to diffuse effectively inside the small pores. It is now commonly believed that CO_2 emissions from burning of fossil fuels in power plants and automobiles are altering the temperature of the atmosphere and the acidity of the oceans with

undesirable consequences for the Earth's environment. It has been shown that MOFs and zeolitic imidazolate frameworks (ZIFs) can hold a large amount of gases, including carbon dioxide, and that gas uptake can be selective. CO_2 uptake of Cu-TBA-3 is comparable to the recently reported ZIF-95, ZIF-100 and BPL carbon[16] (Figure 3 *b*). Although some zeolite materials outperform BPL carbon in terms of selective CO_2 adsorption, then practical use is uncertain because of regeneration difficulties and hence were not included in the comparative adsorption measurements. Figure 3 *b* illustrates that Cu-TBA-3 shows adsorption and desorption of CO_2. More detailed analysis of the data in Figure 3 *b* indicates that 1 g of Cu-TBA-3 can hold 1.64 mmol/g (36.75 cc) CO_2 at 298 K temperature and ambient pressure. Adsorption isotherms for H_2 were collected at 77 K as shown in Figure 5 *a*. It should be noted that the repeatability of the H_2 adsorption behaviour was confirmed by reproducing the same isotherm thrice at 77 K. The uptake at ~ 800 torr at 77 K is 0.69 wt% which is comparable to porous MOFs with small pores. Although H_2 adsorption for Cu-TBA-3 is moderate, they are comparable with H_2 adsorption of highest capacity zeolites, some carbon materials and MOFs reported in the literature.

In conclusion, we have synthesized a new 2D MOF with 1D channels having high porosity. This MOF is highly stable and retains crystallinity until 200°C, which was confirmed by TGA. As in the structure of Cu-TBA-3, owing to narrow pore aperture it is non-porous to N_2, but shows 0.69 wt% and 1.64 mmol/g of H_2 and CO_2 uptake at 77 K and 298 K respectively. This result once again proves that there is an immense potential of synthesizing MOFs with non-carboxylate building blocks, for H_2 and CO_2 uptake properties, using co-ligands. We believe that these findings will not only be useful at the basic level in the crystal engineering of coordination networks but also enrich the database of MOFs having non-carboxylate organic building units. We continue to utilize other neutral

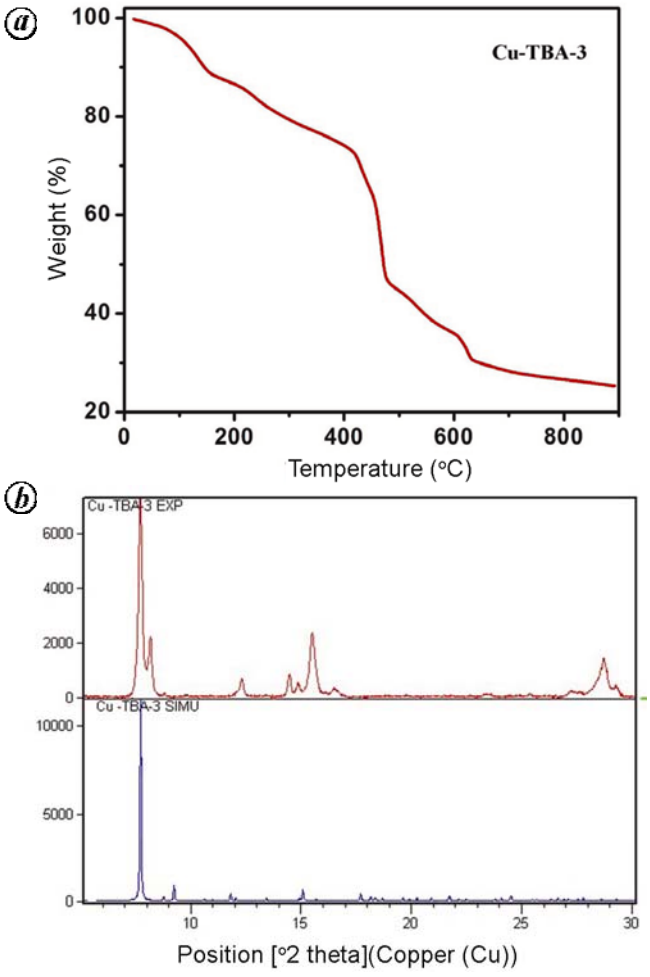

Figure 2. ***a***, Thermogravimetric analysis (TGA) of the Cu-TBA-3 showing gradual weight loss up to 200°C owing to loss of guest DMF molecules. ***b***, Comparison of the experimental PXRD pattern of the synthesized Cu-TBA-3 (top) with the one simulated from its single crystal structure (bottom).

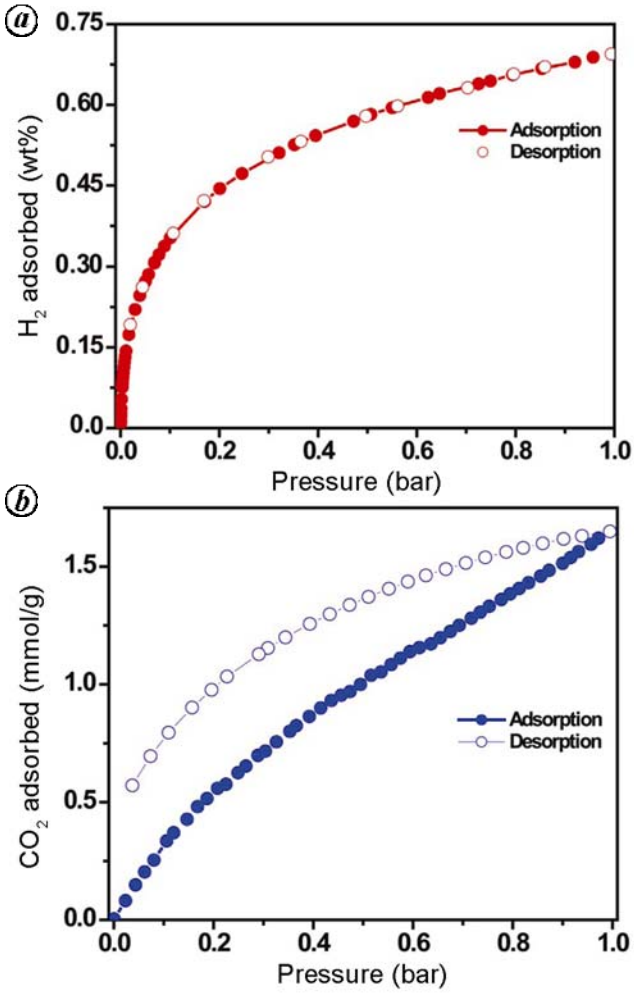

Figure 3. Gas uptake properties of Cu-TBA-3. ***a***, H_2 adsorption isotherms below 1.0 bar for Cu-TBA-3 at 77 K. ***b***, CO_2 adsorption isotherms below 1.0 bar for Cu-TBA-3 at 298 K. Filled and open circles represent adsorption and desorption data, respectively.

bridging co-ligands along with 4-TBA to design new MOFs with specific structures and properties.

Supplementary material available: Supporting information contains description of experimental details including synthetic methods, crystallography, TGA, infrared spectroscopy, powder XRD profiles, tables of crystallographic data, CIF files and anisotropic thermal ellipsoids for MOF reported in this article.

1. Janiak, C., Engineering coordination polymers towards applications. *J. Chem. Soc. Dalton Trans*., 2003, 2781–2804; Moulton, B. and Zaworotko, M. J., From molecules to crystal engineering: Supramolecular isomerism and polymorphism in network solids. *Chem. Rev*., 2001, **101**, 1629–1658; Eddaoudi, M., Moler, D. B., Li, H., Chen, B., Reineke, T. M., O'Keeffe, M. and Yaghi, O. M., Modular chemistry: Secondary building units as a basis for the design of highly porous and robust metal–organic carboxylate frameworks. *Acc. Chem. Res.*, 2001, **34**, 319–330; Robson, R., A net-based approach to coordination polymers. *J. Chem. Soc.*, *Dalton Trans*., 2000, 3735–3744; Yaghi, O. M., Metal–organic frameworks: A tale of two entanglements. *Nat. Mat*., 2007, **6**, 92–93.
2. Eddaoudi, M., Kim, J., Rosi, N., Vodak, D., Wachter, J., O'Keeffe, M. and Yaghi, O. M., Systematic design of pore size and functionality in isoreticular MOFs and their application in methane storage. *Science*, 2002, **295**, 469–472; Kitagawa, S., Kitaura, R. and Noro, S.-I., Functional porous coordination polymers. *Angew. Chem., Int. Ed.*, 2004, **43**, 2334–2375; Matsuda, R. *et al.*, Highly controlled acetylene accommodation in a metal–organic microporous material. *Nature*, 2005, **436**, 238–241.
3. Furukawa, H., Miller, M. A. and Yaghi, O. M., Independent verification of the saturation hydrogen uptake in MOF-177 and establishment of a benchmark for hydrogen adsorption in metal–organic frameworks. *J. Mater. Chem*., 2007, **17**, 3197–3204; Ferey, G., Hybrid porous solids: past, present, future. *Chem. Soc. Rev*., 2008, **37**, 191–214; Ma, S., Sun, D., Simmons, J. M., Collier, C. D., Yuan, D. and Zhou, H.-C., Metal–organic framework from an anthracene derivative containing nanoscopic cages exhibiting high methane uptake. *J. Am. Chem. Soc*., 2008, **130**, 1012–1016.
4. Forster, P. M. and Cheetham, A. K., Hybrid inorganic–organic solids: an emerging class of nanoporous catalysts. *Top. Catal*., 2003, **24**, 79–86; Farrusseng, D., Aguado, S. and Pinel, C., Metal–organic frameworks: Opportunities for catalysis. *Angew. Chem., Int. Ed.*, 2009, **48**, 7502–7513; Wang, Z., Chen, G. and Ding, K., Self-supported catalysts. *Chem. Rev.*, 2009, **109**, 322–359.
5. Horcajada, P. *et al.*, Porous metal–organic-framework nanoscale carriers as a potential platform for drug delivery and imaging. *Nat. Mater.*, 2010, **9**, 172–178; Horcajada, P., Serre, C., Vallet-Regi, M., Sebban, M., Taulelle, F. and Ferey, G., Metal–organic frameworks as efficient materials for drug delivery. *Angew. Chem., Int. Ed.*, 2006, **45**, 5974–5978.
6. Dupuis, A., Guo, N., Gao, Y., Godbout, N., Lacroix, S., Dubois, C. and Skorobogatiy, M., Prospective for biodegradable microstrutured optical fibres. *Opt. Lett*., 2007, **32**, 109–111; Hinks, N. J., McKinlay, A. C., Xiao, B., Wheatley, P. S. and Morris, R. E., Metal organic frameworks as NO delivery materials for biological applications. *Microporous Mesoporous Mater*., 2010, **129**, 330–334; Horcajada, P. *et al*., Flexible porous metal–organic frameworks for a controlled drug delivery. *J. Am. Chem. Soc*., 2008, **130**, 6774–6780.
7. Li, D. and Kaneko, K., Hydrogen bond-regulated microporous nature of copper complex-assembled microcrystals. *Chem. Phys. Lett*., 2001, **335**, 50–56; Bourrelly, S., Llewellyn, P. L., Serre, C., Millange, F., Loiseau, T. and Ferey, G., Different adsorption behaviors of methane and carbon dioxide in the isotypic nanoporous metal terephthalates MIL-53 and MIL-47. *J. Am. Chem. Soc*., 2005, **127**, 13519–13521; Millward, A. R. and Yaghi, O. M., Metal–organic frameworks with exceptionally high capacity for storage of carbon dioxide at room remperature. *J. Am. Chem. Soc*., 2005, **127**, 17998–17999; Ferey, G., Serre, C., Mellot-Draznieks, C., Millange, F., Surble, S., Dutour, J. and Margiolaki, I., A hybrid solid with giant pores prepared by a combination of targeted chemistry, simulation, and powder diffraction. *Angew. Chem*., *Int. Ed*., 2004, **43**, 6296–6301; Ferey, G., Mellot-Draznieks, C., Serre, C., Millange, F., Dutour, J., Surble, S. and Margiolaki, I., A chromium terephthalate-based solid with unusually large pore volumes and surface area. *Science*, 2005, **309**, 2040–2042; Snurr, R. Q., Hupp, J. T. and Nguyen, S. T., Prospects for nanoporous metal–organic materials in advanced separations processes. *AlChE J*., 2004, **50**, 1090–1095.
8. Dillon, A. C., Jones, K. M., Bekkedahl, T. A., Kiang, C. H., Bethune, D. S. and Heben, M. J., Storage of hydrogen in single-walled carbon nanotubes. *Nature*, 1997, **386**, 377–379; Liu, C., Fan, Y. Y., Liu, M., Cong, H. T., Cheng, H. M. and Dresselhaus, M. S., Hydrogen storage in single-walled carbon nanotubes at room temperature. *Science*, 1999, **286**, 1127–1129; Chambers, A., Park, C., Baker, R. T. K. and Rodriguez, N. M., Hydrogen storage in graphite nanofibers. *J. Phys. Chem. B*, 1998, **102**, 4253–4256; Chen, P., Wu, X., Lin, J. and Tan, K. L., High H_2 Uptake by alkali-doped carbon nanotubes under ambient pressure and moderate temperatures. *Science*, 1999, **285**, 91–93.
9. Li, Y. and Yang, R. T., Hydrogen storage in low silica type X zeolites. *J. Phys. Chem. B*, 2006, **110**, 17175–17181; Nijkamp, M. G., Raaymakers, J. E., van Dillen, A. J. and de Jong, K. P., Hydrogen storage using physisorption materials demands. *Appl. Phys. A*, 2001, **72**, 619–623; Darkrim, F., Aoufi, A., Malbrunot, P. and Levesque, D., Hydrogen adsorption in the NaA zeolite: A comparison between numerical simulations and experiments. *J. Chem. Phys*., 2000, **112**, 5991; Yang, R. T., *Adsorbents*: *Fundamentals and Applications*, Wiley, New York, 2003, p. 280.
10. Hynek, S., Fuller, W. and Bentley, J., Hydrogen storage by carbon sorption. *Int. J. Hydrogen Energy*, 1997, **22**, 601–610; Carpetis, C. and Peschka, W., A study on hydrogen storage by use of cryoadsorbents. *Int. J. Hydrogen Energy*, 1980, **5**, 539–554; Noh, J. S., Agarwal, R. K. and Schwarz, J. A., Hydrogen storage systems using activated carbon. *Int. J. Hydrogen Energy*, 1987, **12**, 693–700; Chahine, R. and Bose, T. K., Low-pressure adsorption storage of hydrogen. *Int. J. Hydrogen Energy*, 1994, **19**, 161–164; Zhou, Y. and Zhou, L., Experimental study on high-pressure adsorption of hydrogen on activated carbon. *Sci. China, Ser. B*, 1996, **39**, 598–607; Wang, Q. and Johnson, J. K., Molecular simulation of hydrogen adsorption in single-walled carbon nanotubes and idealized carbon slit pores. *J. Chem. Phys*., 1999, **110**, 577–587; de la Casa-Lillo, M. A., Lamari-Darkrim, F., Cazorla-Amoros, D. and Linares-Solano, A., Hydrogen storage in activated carbons and activated carbon fibers. *J. Phys. Chem. B*, 2002, **106**, 10930–10934; Wang, H., Gao, Q. and Hu, J., High hydrogen storage capacity of porous carbons prepared by using activated carbon. *J. Am. Chem. Soc.*, 2009, **131**, 7016–7022.
11. Das, L. M., On-board hydrogen storage systems for automotive application. *Int. J. Hydrogen Energy*, 1996, **21**, 789–800; Fukai, Y., In *The Metal–Hydrogen System* (ed. Gonser, U.), Springer Series in Material Science, Springer-Verlag, New York, 1993; Imamura, H. and Sakasai, N., Hydriding characteristics of Mg-based composites prepared using a ball mill. *J. Alloys Compd.*, 1995, **231**, 810–814; Imamura, H., Sakasai, N. and Kajii, Y., Hydrogen absorption of Mg-based composites prepared by mechanical milling: Factors affecting its characteristics, *J. Alloys Compd*., 1996, **232**, 218–223; Imamura, H., Sakasai, N. and Fujinaga, T., Characterization and hydriding properties of Mg-graphite composites prepared by mechanical grinding as new hydrogen storage

materials. *J. Alloys Compd.*, 1997, 253–254; Sandrock, G., A panoramic overview of hydrogen storage alloys from a gas reaction point of view. *J. Alloys Compd*., 1999, **293**, 877–888; Schuth, F., Bogdanovi, B. and Felderhoff, M., Light metal hydrides and complex hydrides for hydrogen storage. *Chem. Commun*., 2004, 2249–2258.

12. Morris, R. E. and Wheatley, P. S., Gas storage in nanoporous materials. *Angew. Chem., Int. Ed*., 2008, **47**, 4966–4981; Llewellyn, P. L. *et al*., High uptakes of CO_2 and CH_4 in mesoporous metal organic frameworks MIL-100 and MIL-101. *Langmuir*, 2008, **24**, 7245–7250; Murray, L. J., Dinca, M. and Long, J. R., Hydrogen storage in metal–organic frameworks. *Chem. Soc. Rev*., 2009, **38**, 1294–1314; Chen, B., Xiang, S. and Qian, G., Metal–organic frameworks with functional pores for recognition of small molecules. *Acc. Chem. Res*., 2010, **43**, 1115–1124.
13. Zhang, J. P., Lin, Y.-Y., Zhang, W.-X. and Chen, X.-M., Copper(I) 1,2,4-triazolates and related complexes: Studies of the solvothermal ligand reactions, network topologies, and photoluminescence properties. *J. Am. Chem. Soc*., 2005, **127**, 5495–5506; Patel, R., Weller, M. T. and Price, D. J., Topological ferrimagnetism and superparamagnetic-like behaviour in a dissordered homometalic coordination network. *Dalton Trans.*, 2007, 4034–4039; Wang, Y., Ding, B., Cheng, P., Liao, D.-Z. and Yan, S.-P., Tuned triazolatesilver(I) luminescent complexes from zero- to three-dimensionality based on bi- to tetratopic bridged ligands. *Inorg. Chem*., 2007, **46**, 2002–2010; Dinca, M., Dailly, A., Tsay, C. and Long, J. R., Expanded sodalite-type metal–organic frameworks: increased stability and H_2 adsorption through ligand-directed catenation. *Inorg. Chem.*, 2008, **47**, 11–13; Zhang, J.-P. and Chen, X. M., Crystal engineering of binary metal imidazolate and triazolate frameworks. *Chem. Commun*., 2006, 1689–1699; Zhao, H., Qu, Z.-R., Ye, H.-Y. and Xiong, R.-G., *In situ* hydrothermal synthesis of tetrazole coordination polymers with interesting physical properties. *Chem. Soc. Rev*., 2008, **37**, 84–100; Pachfule, P., Das, R., Poddar, P. and Banerjee, R., Structural, magnetic, and gas adsorption study of a two-dimensional tetrazole-pyrimidine based metal–organic framework. *Cryst. Growth. Des*., 2010, **10**, 2475–2478; Pachfule, P., Chen, Y., Jiang, J. and Banerjee, R., Structural isomerism and effect of fluorination on gas adsorption in copper-tetrazolate based metal organic frameworks. *Chem. Mater*., 2011, **13**, 2908–2916.
14. Koyama, M., Ohtani, N., Kai, F., Moriguchi, I. and Inouye, S., Synthesis and quantitative structure-activity relationship analysis of N-triiodoallyl- and N-iodopropargylazoles, new antifungal agents. *J. Med. Chem*., 1987, **30**, 552–562.
15. Spek, A. L., PLATON, *A Multipurpose Crystallographic Tool*, Utrecht University, Utrecht, The Netherlands, 2005.
16. Park, K. S. *et al*., Exceptional chemical and thermal stability of zeolitic imidazolate frameworks. *Proc. Natl. Acad. Sci. USA*, 2006, **103**, 10186–10191; Zhou, W., Wu, H., Hartman, M. R. and Yildirim, T., Hydrogen and methane adsorption in metal–organic frameworks: A high-pressure volumetric study. *J. Phys. Chem. C*, 2007, **111**, 16131–16137; Chen, B. L., Ma, S. Q., Hurtado, E. J., Lobkovsky, E. B. and Zhou, H. C., A triply interpenetrated microporous metal–organic framework for selective sorption of gas molecules. *Inorg. Chem*., 2007, **46**, 8490–8492; Chen, B. L. *et al*., A microporous metal–organic framework for gas-chromatographic separation of alkanes. *Angew. Chem., Int. Ed*., 2006, **45**, 1390–1393; Wong-Foy, A. G., Matzger, A. J. and Yaghi, O. M., Exceptional H_2 saturation uptake in microporous metal–organic frameworks. *J. Am. Chem. Soc*., 2006, **128**, 3494–3495; Rowsell, J. L. C. and Yaghi, O. M., Effects of functionalization, catenation, and variation of the metal oxide and organic linking units on the low-pressure hydrogen adsorption properties of metal–organic frameworks. *J. Am. Chem. Soc*., 2006, **128**, 1304–1315; Dailly, A., Vajo, J. J. and Ahn, C. C., Saturation of hydrogen sorption in Zn benzenedicarboxylate and Zn naphthalenedicarboxylate. *J. Phys. Chem. B*, 2006, **110**, 1099–1101; Zhao, D., Yuan, D. and Zhou, H.-C., The current status of hydrogen storage in metal–organic frameworks. *Energy Environ. Sci*., 2008, **1**, 222–235.

ACKNOWLEDGEMENTS. P.P. thanks CSIR for project assistantship (PA-II) from CSIR's XI Five Year Plan Project. R.B. thanks Dr S. Pal, Director NCL for in-house project and CSIR's XI Five Year Plan Project and Clean Coal Technology Project for funding and also Drs B. D. Kulkarni, S. Sivaram and K. Vijaymohanan for their encouragement. Financial assistance from the DST is gratefully acknowledged.